Published in final edited form as:

Cell Rep. 2018 August 07; 24(6): 1456–1463. doi:10.1016/j.celrep.2018.07.015.

Body Cavity Development Is Guided by Morphogen Transfer between Germ Layers

Jan Schlueter[1] and **Takashi Mikawa**[1,2,*]

[1]University of California San Francisco, School of Medicine, Cardiovascular Research Institute, 555 Mission Bay Blvd South, San Francisco, CA 94158, USA

[2]Lead Contact

SUMMARY

The body cavity is a space where internal organs develop and are placed. Despite the importance of this internal space, how the body cavity forms specifically within the mesoderm remains largely unknown. Here, we report that upon the onset of dorsal mesodermal cell polarization and initial lumen formation, mesodermal cells form filamentous projections that are directed toward the ectoderm. This cell behavior enables the dorsal population of mesodermal cells to receive BMP7 that is expressed by the ectoderm. Suppression of ectodermal BMP7 diminishes mesodermal cell projection and results in the loss of body cavity development. The data reveal that body cavity induction depends on signaling factor transfer from ectoderm to mesoderm.

Graphical Abstract

*Correspondence: takashi.mikawa@ucsf.edu.

AUTHOR CONTRIBUTIONS

T.M. and J.S. designed the research and wrote the paper, and J.S. performed the experiments.

SUPPLEMENTAL INFORMATION

Supplemental Information includes four figures and four videos and can be found with this article online at https://doi.org/10.1016/j.celrep.2018.07.015.

DECLARATION OF INTERESTS

The authors declare no competing interests.

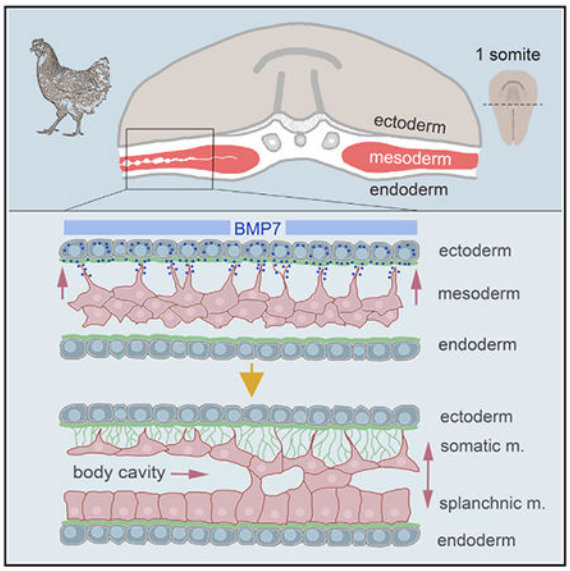

In Brief

Schlueter and Mikawa show that body cavity formation is initiated by mesodermal cell projections that are directed toward the ectoderm. These projections are promoted by ectodermal BMP7, which plays a crucial role in the establishment of two distinct mesodermal layers at the onset of body cavity development.

INTRODUCTION

The body cavity or coelom is highly conserved among bilaterians and takes place within the mesoderm during early embryogenesis (Morris, 2016; Gruhl et al., 2009). The naive lateral plate mesoderm differentiates into two layers along the dorsoventral axis (Maggert et al., 1995; Meier, 1980). The somatic mesoderm establishes dorsally and the visceral or splanchnic mesoderm establishes ventrally the inner cavity lining throughout the body to support internal organ development and placement (Azpiazu et al., 1996; Bishopric, 2005). Paracrine interactions of the mesoderm with the ectoderm and endoderm pattern mesodermal morphogenesis and differentiation. However, our understanding of molecular and cell biological mechanisms that regulate the initiation of cavity formation within the mesoderm remains rudimentary.

Several mechanisms have been suggested for lumen formation during embryonic development. These include hollowing out existing tissues, for example, by generation of intracellular vacuoles to form vascular structures (Kamei et al., 2006); osmolality changes by ion channels (Ferrari et al., 2008); and apoptosis to hollow out the mouse blastula during early implantation stages (Penaloza et al., 2006).

In this study, we identify distinct morphogenetic mechanisms of cavity formation in the native lateral plate mesoderm. Using high-resolution bi-photonic live imaging of transgenic chicken embryos, we show that the body cavity is induced in the mesoderm by transfer of

signaling molecules, such as BMP7, from the ectoderm. This morphogen transfer is mediated through mesodermal cell projections that resemble cytonemes (Ramírez-Weber and Kornberg, 1999; Roy et al., 2014; Kornberg, 2014) and dynamically extend and retract with the ectoderm. The maintenance of mesodermal cell projections depends on ectodermal BMP7 in an indirect manner. These findings provide new insight for cellular mechanisms underlying germ layer cooperation for body cavity induction and development.

RESULTS

To investigate body cavity formation in the embryo, we established a comprehensive live imaging approach (Figure 1; Video S1), combined with a cryosection-based histological analysis. We used the chick embryo, whose relatively simple flat configuration facilitates live imaging. During early, presomitic stages of body cavity formation (Hamburger-Hamilton stage [HH] 6) (Hamburger and Hamilton, 1951), the lateral plate mesoderm consists of mesenchymal cells that are sandwiched between two epithelial sheets: the underlying endoderm and the overlying ectoderm. If not indicated otherwise, all sections shown represent the level of the first somite pair. To study the onset of cavity formation and epithelization of mesodermal cells, we monitored apicobasal polarity in the three germ layers using the basal marker Laminin1. Laminin1 was detected at the basal side of both ectoderm and endoderm where they face the mesoderm (Figures 1A–1D).

Before overt lumen formation, mesodermal cells became polarized as indicated by apical enrichment of filamentous actin (F-actin). At this developmental stage, other apical markers such as N-cadherin were reproducibly detected only in the anterior heart-forming region of the embryo and therefore are not used in this study. Accumulation of F-actin generated a demarcation within the lateral plate that indicated the future apical side of mesodermal cells (Figure 1B). At the one somite stage (HH7), overt lumen formation within the lateral mesoderm first became evident as small isolated cavities. At the 4-somite stage (HH8), smaller cavities (average diameter 49 ± 7.2 μm, mean ± SEM) were fused into larger cavities that spanned up to 120 μm on average ± 18.6 μm (SEM) across the dorsoventral axis. This lumen formation gradually progressed from lateral to medial across the lateral plate mesoderm (Figures 1A–1D).

To elucidate mechanisms that regulate body cavity formation, we developed a new live imaging approach for high-resolution transverse optical slices of the anterior halves of EGFP-expressing chicken embryos (Chapman et al., 2005) using two-photon microscopy (Figures 1E and 1F). The resolution along the dorsoventral axis was higher than a conventional scan axis and was sufficient to visualize fine cellular projections between the mesoderm and the ectoderm (Figures 1G and 1H). Within time windows up to 3 hr, this imaging protocol revealed that the dorsal portion of mesodermal cells dynamically generated many cellular projections toward the dorsal ectoderm before and concomitant with initial lumen formation (Figures 1H and 2A–2D; Videos S1 and S2).

The gradual opening of small mesodermal cavities and progressive fusion into larger cavities across the medial-lateral embryonic axis was also detected (Figures 2C, 2D, and 2M; Video S1). During cell projection activity, the dorsal mesoderm reorganized into a continuous cell

layer below the ectoderm. The live imaging data revealed that the surface of dorsal mesodermal cells exposed to the ectoderm had many cellular protrusions (Figures 2E–2H; Videos S1 and S2). While extending and retracting over the course of 15 min, these cellular projections reach a length of about 38 μm with an average length of 26.16 ± 5.06 μm (mean ± SEM) and bridge the gap between mesoderm and ectoderm (Figures 2E–2H, 2N, and 2O). We tracked mesodermal cell projections over the course of 45 min in 5 min steps and observed an average of18 cell projections per 0.01 cm^2 (Figures 2E–2H, 2N, and 2O; Video S2).

Analysis of sections by confocal microscopy also identified mesodermal projections that extend toward the ectoderm (Figures 2I–2L). These cellular projections predominantly oriented toward the basal side of the ectoderm. In some cases, cell extensions displayed branching and reached to the ectoderm at different points (Figures 2I–2L). These projections contained F-actin (Figures 2I–2L), as well as α-tubulin (Figures 1A–1D and 2I–2L). Because the cellular projections resembled cytonemes or long filopodia for cell-to-cell signaling in the *Drosophila* wing disc (Ramírez-Weber and Kornberg, 1999) and other systems (Sagar et al., 2015; Sanders et al., 2013; Stanganello et al., 2015), we suspected that these projections had a role in a tissue-tissue interaction regulating the initiation of body cavity formation. We tested this possibility by examining the distribution of ectodermal BMP7, a key molecular signal for the dorsoventral patterning of the mesoderm (Funayama et al., 1999). To visualize ectodermally produced BMP7 protein during body cavity formation, we introduced a human bone morphogenetic protein 7 (hBMP7)-FLAG construct into the ectoderm traced the tagged BMP7 (n = 10) (Figures 3A–3D). The originally transfected cell population was determined by co-electroporation with a lissamine rhodamine (LRSC)-labeled control DNA oligomer (oligo), demonstrating the construct was successfully and exclusively introduced to the ectodermal cells (Figures 3G and 3K). After 8 hr, anti-FLAG immunohistochemistry detected the tagged BMP7 protein in mesodermal projections that protruded toward the ectoderm. It was not detected in a cellular areas in the surrounding matrix (Figures 3E, 3F, 3I, and 3J). The mesoderm cells that carried the hBMP7-FLAG protein were negative for the transfection control LRSC-tagged DNA oligo (Figure 3), demonstrating that this exogenous DNA does not reach to mesodermal cells by this transfection method. The apparent absence of hBMP7-FLAG in the extracellular space between the mesoderm and the ectoderm suggests that mesodermal cells received the FLAG-tagged BMP7 directly from the ectoderm. In control experiments in which a vector only expressing a FLAG tag was co-electroporated, together with the transfection control LRSC oligo, the FLAG tag was not detected in mesodermal cells, despite the presence of actin-containing projections protruding toward the ectoderm (n = 9) (Figures 3M–3T; Figure S1). The data are consistent with the idea of cell contact-dependent cytokine delivery, although they do not rule out the possibility of indirect uptake of BMP7 from extracellular space.

The sides of embryos that overexpressed hBMP7 had larger cavities than the untreated sides (n = 6). The enlarged cavities extended into posterior areas that would not normally have a discernable lumen at this stage (Figures 3U–3W). These data suggested that ectodermal BMP7 has a positive influence on body cavity formation in the lateral plate mesoderm (Figures 3U–3W). Furthermore, activin receptor IIA (ActRII2A), which is necessary for BMP7 signaling, is expressed in dorsal mesodermal cells (Figure S2). To test whether BMP7

is required, we reduced ectodermal BMP7 levels by introducing an antisense morpholino against BMP7 selectively to the ectoderm (n = 18). Live imaging at the onset of body cavity formation revealed a severe reduction of mesodermal projection activity in comparison to controls (n = 25) (Figures 4A–4C; Videos S3 and S4), and the lateral plate mesoderm did not generate two separate cell layers or generate a discernible cavity. Although mesodermal cells had indications of apicobasal polarization (Figures 4G–4I), analysis of Laminin1 expression suggested that epithelialization of the dorsal subpopulation of the lateral plate mesoderm failed (Figures 4D–4I). In contrast to controls, Laminin1 was largely absent from dorsal mesodermal cells, although the ventral mesoderm seemed to express normal levels of Laminin1 and a typical columnar pseudostratified epithelial morphology. Fibronectin, which was expressed in the ectoderm and deposited between mesoderm and ectoderm, was also reduced after this treatment (Figure S4). Histological analysis confirmed our observations from live imaging experiments, because control embryos displayed long mesodermal projections extending toward the ectoderm and strongly localizing with Laminin1 (Figures 4E and 4F), while these projections had mostly disappeared in loss-of-BMP7 embryos (Figures 4H and 4I). To test for specificity in a rescue experiment, the BMP7 antisense morpholino was co-electroporated, together with an RNA that coded for FLAG-tagged human BMP7 but was not complementary to the antisense morpholino (n = 8). After this treatment, the mesoderm developed into two separate layers and the body cavity fully developed in comparison to the untreated side of the embryo, indicating that the rescue was successful (Figure S3). These data suggest that signaling between ectoderm and lateral plate mesoderm directly affects body cavity morphogenesis.

DISCUSSION

Our data are consistent with a model wherein ectodermal BMP7 protein is received by the mesoderm via cellular projections and this receipt of BMP7 is critical for mesodermal patterning (Figure 4J). Cellular extensions or filopodia have long been described and associated with dynamic events like cell migration and wound healing (Mattila and Lappalainen, 2008). Studies have demonstrated additional roles for filopodia or filopodia-like extensions that are enriched with F-actin. In *Drosophila*, filopodia-like extensions, or cytonemes, are responsible for transporting morphogens like decapentaplegic (DPP) to distant cells (Roy et al., 2014). Our data suggest that filopodia-mediated transfer of ligands produced by this gene family is conserved in vertebrates.

Our experiments do not reveal whether the projections of mesodermal cells that extend to the ectoderm are induced directly by BMP7, and little is known about the factors that influence the initiation or orientation of cellular projections or cytonemes in other contexts. One model suggests that there is a continuous scanning of the surrounding area by cytonemes (Kornberg and Roy, 2014). In this model, cytonemes are a normal interaction of cell with environment, and they are stabilized when signals are encountered. Our data suggest that BMP7 induces a specific environment or niche that facilitates mesodermal filopodia activity, because we observe a reduction of extracellular matrix between ectoderm and mesoderm after loss of BMP7. It is plausible that ectodermal BMP7 plays a vital role for a projection-friendly environment and is taken up by mesodermal cells to form cavities. Data indicate that the extracellular matrix environment is crucial for filopodia activity (Huang and

Kornberg, 2016; Sato et al., 2017). In addition, it remains to be determined how mesodermal projections receive ligands like BMP7 and whether the ligand need to secreted or can be taken up, because the mesodermal projection might also fuse with the ectodermal cell membrane.

Although bone morphogenetic proteins (BMPs) are known to induce mesoderm and specify mesodermal fate (Dale and Jones, 1999), our interference with BMP7 in the ectoderm had no effect on the expression of somatic mesodermal markers like Twist1 (Figures S4Q and S4R). We conclude that BMP2 in the ectoderm and BMP4 in the mesoderm that were not targeted in our experiments are sufficient to induce somatic mesodermal fate.

Our high-resolution bi-photonic live imaging revealed that the body cavity is induced in the mesoderm by cytoneme-like projection-mediated transfer of BMP7 from the ectoderm. The body cavity morphogenesis is clearly distinct from several known mechanisms for lumen formation during embryonic development: hollowing out existing tissues, for example, by generation of intracellular vacuoles to form vascular structures (Kamei et al., 2006); osmolality changes by ion channels (Ferrari et al., 2008); and apoptosis to hollow out the mouse blastula during early implantation stages (Penaloza et al., 2006). Although we examined various stages during body cavity formation, our study detected no evidence for any of these mechanisms (Figures S4M–S4P).

Although the formation of a body cavity is highly conserved, there is little mechanistic and molecular insight into how lumen formation is induced in the lateral plate mesoderm. Although in *Drosophila* the dorsal spreading of future somatic mesoderm might involve DPP (McMahon et al., 2010), this study provides evidence that BMP plays an important role in the body cavity formation of higher vertebrates.

After the body cavity has formed, derivatives of the lateral plate mesoderm, such as the heart, the vasculature, the limbs, and serous mesothelial membranes, can develop (Kelly et al., 2014; Callebaut et al., 2004; Onimaru et al., 2011; Nishimoto and Logan, 2016; Ariza et al., 2016; Schlueter and Brand, 2013). Deeper investigation of the formation of the body cavity as a conserved feature of the animal kingdom will not only further our knowledge about the initiation of organogenesis but also help unravel general mechanisms underlying how tissues influence and pattern one another.

EXPERIMENTAL PROCEDURES

Embryology

Chicken embryos were obtained by incubating eggs from *Gallus gallus domesticus* to the desired stages between 24 and 36 hr at 37°C. For manipulative experiments, chicken embryos were cultivated on filter papers in bacto agar plates according to the early chick (EC) culture protocol (Chapman et al., 2001)

Electroporation and Histology

Embryos were transfected with vector DNA and morpholino DNA using the Nepagene NEPA21 type II electroporator with 4 pulses of 5 Volt, 20 ms duration, and 200 ms interval.

Platinum electrodes were used and placed over and under the cultivated embryo while avoiding direct tissue contact. The injection mix contained 0.1% fast green, 0.5% methylcellulose, and 5 μg/μL DNA. Embryos were processed for histology by fixation in 4% paraformaldehyde (PFA), washed twice with PBS, and prepared for cryohistology. Embryos were frozen in optimal cutting temperature (OCT) compound (Tissue-Tek, 4583) and 14 μm thick sections were generated on a cryotome.

Immunohistochemistry and Microscopy

Primary antibodies were used in the following dilutions: anti-FLAG M2 mouse monoclonal 1:100 (F1804, Sigma), α-tubulin mouse monoclonal 1:1,000 (T6199, Sigma), and laminin rabbit polyclonal 1:100 (L9393, Sigma). Secondary antibodies and phalloidin were used in the following dilutions: Alexa 488 rabbit 1:1,000 (A11008, Invitrogen, Molecular Probes), Alexa 594 mouse 1:1,000 (A21125, Invitrogen, Molecular Probes), and Phalloidin 635 1:200 (A34054, Thermo Fisher Scientific). Tissue sections were subsequently analyzed using the confocal microscope Leica SPE.

Live Imaging

GFP-expressing embryos (commercially available from Clemson University, South Carolina) (Chapman et al., 2005) were cut in half, and the anterior half was mounted in a block of 1.2% low melting agarose in Pannett Compton buffer. The chick embryos uniformly express EGFP under the control of a phosphoglycerate kinase (PGK) promoter. The block was glued on a 35 mm culture dish and filled with buffer to avoid desiccation and enable use of the upright water dipping lenses of a Zeiss LSM 7 MP. Embryos were scanned for up to 3 hr. 3D and 4D analyses were performed in Imaris 8.3.

Whole-Mount *In Situ* Hybridization

According to D.G. Wilkinson, antisense RNA probes labeled with digoxigenin (Roche) were generated against ActRIIA by linearizing with PvuII and transcribing with T3 polymerase (Promega) (Stern et al., 1995, received from Janet Hyer).

Vectors and Morpholinos

The humanBMP73xFLAG construct was bought from Vectorbuilders. The pCAG-GFP was a gift from Connie Cepko (Addgene plasmid 11150). The morpholinos were bought from Gene Tools. BMP7: 5′-CCGGGATGCCCTATACT CACCACCA-3′, BMP7 control: 5′-CCCGGATCCCCTATAATCACAACAA-3′, standard control: 5′-CCTCTTACCTCAGTTACAATTTATA-3′.

Supplementary Material

Refer to Web version on PubMed Central for supplementary material.

ACKNOWLEDGMENTS

We thank Thomas Kornberg for his suggestions on the manuscript. We also thank Lisandro Maya-Ramos, Sara Venters, Jeanette Hyer, and Angela Torlopp for carefully reading the manuscript and for their suggestions. This

work has been funded by NIH NHLBI R37HL07892, NIH NHLBI R01HL122375, and NIH NHLBI R01HL132832.

REFERENCES

Ariza L, Carmona R, Cañete A, Cano E, and Muñoz-Chápuli R (2016). Coelomic epithelium-derived cells in visceral morphogenesis. Dev. Dyn 245, 307–322. [PubMed: 26638186]

Azpiazu N, Lawrence PA, Vincent JP, and Frasch M (1996). Segmentation and specification of the *Drosophila* mesoderm. Genes Dev 10, 3183–3194. [PubMed: 8985186]

Bishopric NH (2005). Evolution of the heart from bacteria to man. Ann. N Y Acad. Sci 1047, 13–29. [PubMed: 16093481]

Callebaut M, Van Nueten E, Bortier H, and Harrisson F (2004). Induction of the avian coelom with associated vitelline blood circulation by Rauber's sickle derived junctional endoblast and its fundamental role in heart formation. J. Morphol 259, 21–32. [PubMed: 14666522]

Chapman SC, Collignon J, Schoenwolf GC, and Lumsden A (2001). Improved method for chick whole-embryo culture using a filter paper carrier. Dev. Dyn 220, 284–289. [PubMed: 11241836]

Chapman SC, Lawson A, Macarthur WC, Wiese RJ, Loechel RH, Burgos-Trinidad M, Wakefield JK, Ramabhadran R, Mauch TJ, and Schoenwolf GC (2005). Ubiquitous GFP expression in transgenic chickens using a lentiviral vector. Development 132, 935–940. [PubMed: 15673573]

Dale L, and Jones CM (1999). BMP signalling in early *Xenopus* development. BioEssays 21, 751–760. [PubMed: 10462415]

Ferrari A, Veligodskiy A, Berge U, Lucas MS, and Kroschewski R (2008). ROCK-mediated contractility, tight junctions and channels contribute to the conversion of a preapical patch into apical surface during isochoric lumen initiation. J. Cell Sci 121, 3649–3663. [PubMed: 18946028]

Funayama N, Sato Y, Matsumoto K, Ogura T, and Takahashi Y (1999). Coelom formation: binary decision of the lateral plate mesoderm is controlled by the ectoderm. Development 126, 4129–4138. [PubMed: 10457021]

Gruhl A, Wegener I, and Bartolomaeus T (2009). Ultrastructure of the body cavities in Phylactolaemata (Bryozoa). J. Morphol 270, 306–318. [PubMed: 19107820]

Hamburger V, and Hamilton HL (1951). A series of normal stages in the development of the chick embryo. J. Morphol 88, 49–92. [PubMed: 24539719]

Huang H, and Kornberg TB (2016). Cells must express components of the planar cell polarity system and extracellular matrix to support cytonemes. eLife 5, e18979. [PubMed: 27591355]

Kamei M, Saunders WB, Bayless KJ, Dye L, Davis GE, and Weinstein BM (2006). Endothelial tubes assemble from intracellular vacuoles *in vivo*. Nature 442, 453–456. [PubMed: 16799567]

Kelly RG, Buckingham ME, and Moorman AF (2014). Heart fields and cardiac morphogenesis. Cold Spring Harb. Perspect. Med 4, a015750. [PubMed: 25274757]

Kornberg TB (2014). Cytonemes and the dispersion of morphogens. Wiley Interdiscip. Rev. Dev. Biol 3, 445–463. [PubMed: 25186102]

Kornberg TB, and Roy S (2014). Cytonemes as specialized signaling filopodia. Development 141, 729–736. [PubMed: 24496611]

Maggert K, Levine M, and Frasch M (1995). The somatic-visceral subdivision of the embryonic mesoderm is initiated by dorsal gradient thresholds in *Drosophila*. Development 121, 2107–2116. [PubMed: 7635056]

Mattila PK, and Lappalainen P (2008). Filopodia: molecular architecture and cellular functions. Nat. Rev. Mol. Cell Biol 9, 446–454. [PubMed: 18464790]

McMahon A, Reeves GT, Supatto W, and Stathopoulos A (2010). Mesoderm migration in *Drosophila* is a multi-step process requiring FGF signaling and integrin activity. Development 137, 2167–2175. [PubMed: 20530544]

Meier S (1980). Development of the chick embryo mesoblast: pronephros, lateral plate, and early vasculature. J. Embryol. Exp. Morphol 55, 291–306. [PubMed: 7373199]

Morris VB (2016). Analysis of coelom development in the sea urchin *Holopneustes purpurescens* yielding a deuterostome body plan. Biol. Open 5, 348–358. [PubMed: 26892238]

Nishimoto S, and Logan MP (2016). Subdivision of the lateral plate mesoderm and specification of the forelimb and hindlimb forming domains. Semin. Cell Dev. Biol 49,102–108. [PubMed: 26643124]

Onimaru K, Shoguchi E, Kuratani S, and Tanaka M (2011). Development and evolution of the lateral plate mesoderm: comparative analysis of amphioxus and lamprey with implications for the acquisition of paired fins. Dev. Biol 359, 124–136. [PubMed: 21864524]

Penaloza C, Lin L, Lockshin RA, and Zakeri Z (2006). Cell death in development: shaping the embryo. Histochem. Cell Biol 126, 149–158. [PubMed: 16816938]

Ramírez-Weber FA, and Kornberg TB (1999). Cytonemes: cellular processes that project to the principal signaling center in *Drosophila* imaginal discs. Cell 97, 599–607. [PubMed: 10367889]

Roy S, Huang H, Liu S, and Kornberg TB (2014). Cytoneme-mediated contact-dependent transport ofthe *Drosophila* decapentaplegic signaling protein. Science 343, 1244624. [PubMed: 24385607]

Sagar, Pröls F, Wiegreffe C, and Scaal M (2015). Communication between distant epithelial cells by filopodia-like protrusions during embryonic development. Development 142, 665–671. [PubMed: 25617437]

Sanders TA, Llagostera E, and Barna M (2013). Specialized filopodia direct long-range transport of SHH during vertebrate tissue patterning. Nature 497, 628–632. [PubMed: 23624372]

Sato Y, Nagatoshi K, Hamano A, Imamura Y, Huss D, Uchida S, and Lansford R (2017). Basal filopodia and vascular mechanical stress organize fibronectin into pillars bridging the mesoderm-endoderm gap. Development 144, 281–291. [PubMed: 28096216]

Schlueter J, and Brand T (2013). Subpopulation of proepicardial cells is derived from the somatic mesoderm in the chick embryo. Circ. Res 113, 1128–1137. [PubMed: 24019406]

Stanganello E, Hagemann AI, Mattes B, Sinner C, Meyen D, Weber S, Schug A, Raz E, and Scholpp S (2015). Filopodia-based Wnt transport during vertebrate tissue patterning. Nat. Commun 6, 5846. [PubMed: 25556612]

Stern CD, Yu RT, Kakizuka A, Kintner CR, Mathews LS, Vale WW, Evans RM, and Umesono K (1995). Activin and its receptors during gastrulation and the later phases of mesoderm development in the chick embryo. Dev. Biol 172, 192–205. [PubMed: 7589799]

Highlights

- Live visualization of early body cavity formation and mesodermal cell behavior
- Mesodermal cells form long projections and reach out toward surface ectoderm
- Ectodermal BMP7 is delivered to mesodermal cells via cellular projections
- BMP7 is crucial for body cavity formation by promoting mesodermal epithelization

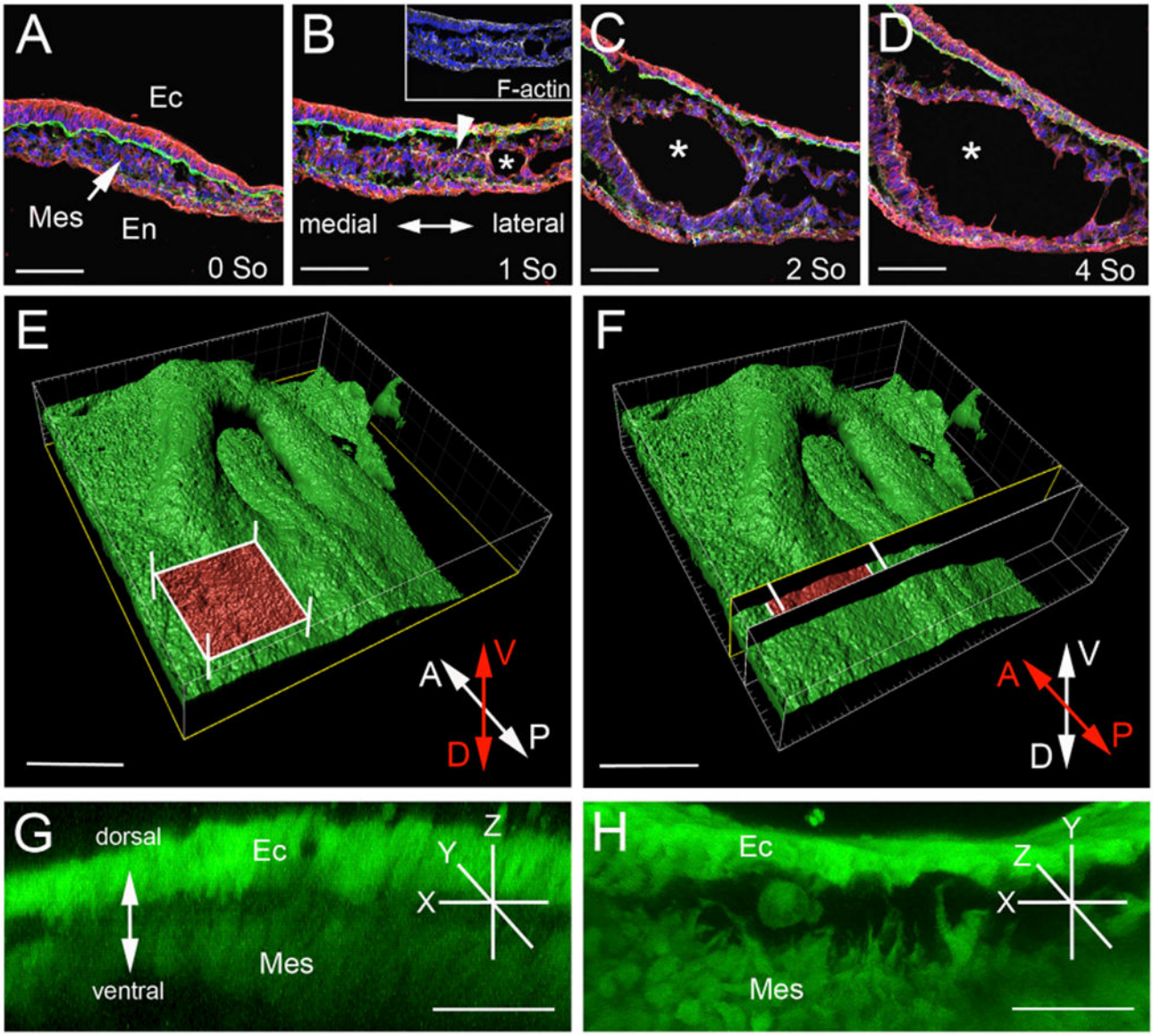

Figure 1. Body Cavity Formation Analysis by Cryohistology and Live Imaging Approaches

(A–D) Lateral plate mesoderm at the 0-somite stage (A), α-tubulin expression in red, Laminin1 deposition in green, F-actin deposition in white and nuclei in blue. At the 1-somite stage (HH7) (B), first cavities within the mesoderm can be detected (asterisk), and F-actin enrichment labels a demarcation line in the mesoderm along which cavity formation is initiated (arrow). (C and D) Mesoderm continues to form two layers. Scale bars: 50 μm.

(E) Whole-mount three-dimensional reconstruction of an anterior chick embryo half at the 4-somite stage. The red square indicates the area of interest in the lateral plate where body cavity formation is occurring. The area is scanned along the dorsoventral axis in an embryo culture dish. Scale bar: 300 μm.

(F) Embryo semiculture configuration. Scale bar: 300 μm.

(G) Conventional dorsoventral scan displays distortions and low resolution along the z axis. Scale bar: 30 μm.

(H) z axis is originally scanned along the anteroposterior axis, which results in enhanced resolution along the dorsoventral axis. Scale bar: 30 μm.

A, anterior; D, dorsal; P, posterior; V, ventral; Ec, ectoderm; En, endoderm; Mes, mesoderm; So, so mites.

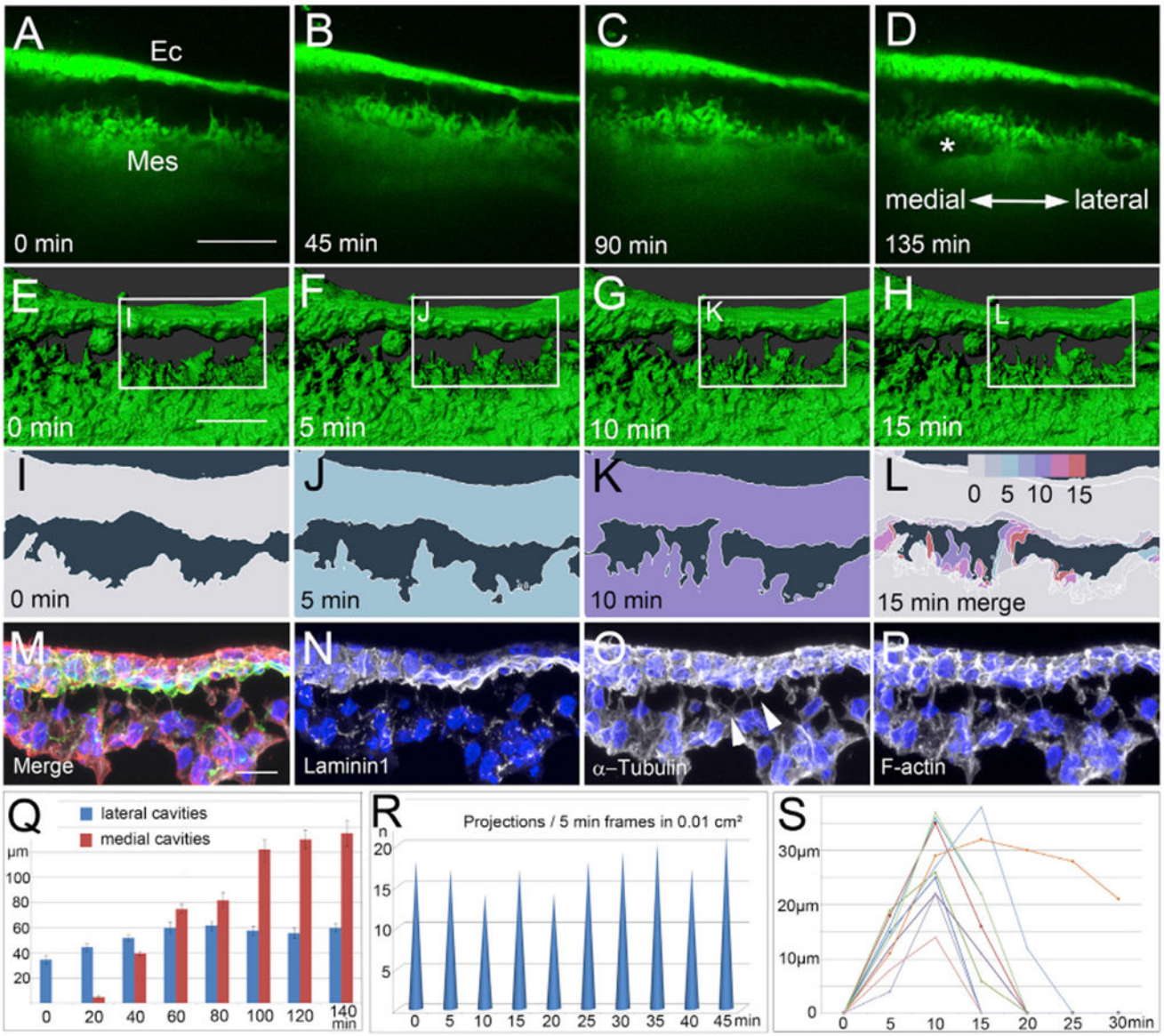

Figure 2. Live Imaging Analysis of Mesodermal Cell Behavior during Body Cavity Formation and Immunohistochemistry

(A) Transverse optical slice through lateral plate mesoderm of a 1-somite stage GFP-expressing chick embryo. Mesodermal cells dynamically project long extensions toward the ectoderm during body cavity initiation. Scale bar: 100 μm.

(B–D) Smaller cavities are formed within the mesoderm and subsequently fuse into larger cavities (asterisk). Time recorded is indicated. The mesoderm continues to project fine cellular extensions toward the ectoderm.

(E–H) Three-dimensional rendering of cell interactions between mesoderm and ectoderm. Time recorded is indicated. Scale bar: 30 μm.

(I–L) Color-coded timeframes depicting tissue silhouettes reveal the dynamics of cell projections over a period of 15 min. Time recorded is indicated. (L) Overlay of 4 frames of

color-coded tissue silhouettes. White represents the starting frame, cyan the 5 min frame, purple the 10 min frame and red the 15 min frame.

(M) Subarea showing mesodermal projections to the ectoderm in an overlayof4channels, with α-tubulin in red, Laminin1 in green, F-actin in white, and nuclei in blue. Mesodermal protrusions are based on F-actin and α-tubulin. Scale bar: 10 μm.

(N–P) Separate channels overlay with blue nuclei. (N) Ectodermal Laminin1 deposition serves as the interface for mesodermal cells. (O and P) Mesodermal cell projections contain α-tubulin (O) and F-actin (P) and are oriented toward the ectoderm and display branching (white arrows).

(Q) Size development of medial and lateral cavities over time in 2-somite embryos, with the section plane on the 1-somite level (accumulative data from 3 embryos, measurements per time point n = 6, total n = 18/time point).

(R) Monitoring mesodermal cell activity in 5 min steps over a period of 45 min in a region the size of 0.01 cm^2 detects an average of 18 mesodermal projections per 5 min frame toward the ectoderm.

(S) On average, individual mesodermal cell projections extend and retract over a period of 15 to 20 min with a length of up to 38 μm and an average length of 26.16 ± 5.06 μm (mean ± SEM).

See also Videos S1 and S2.

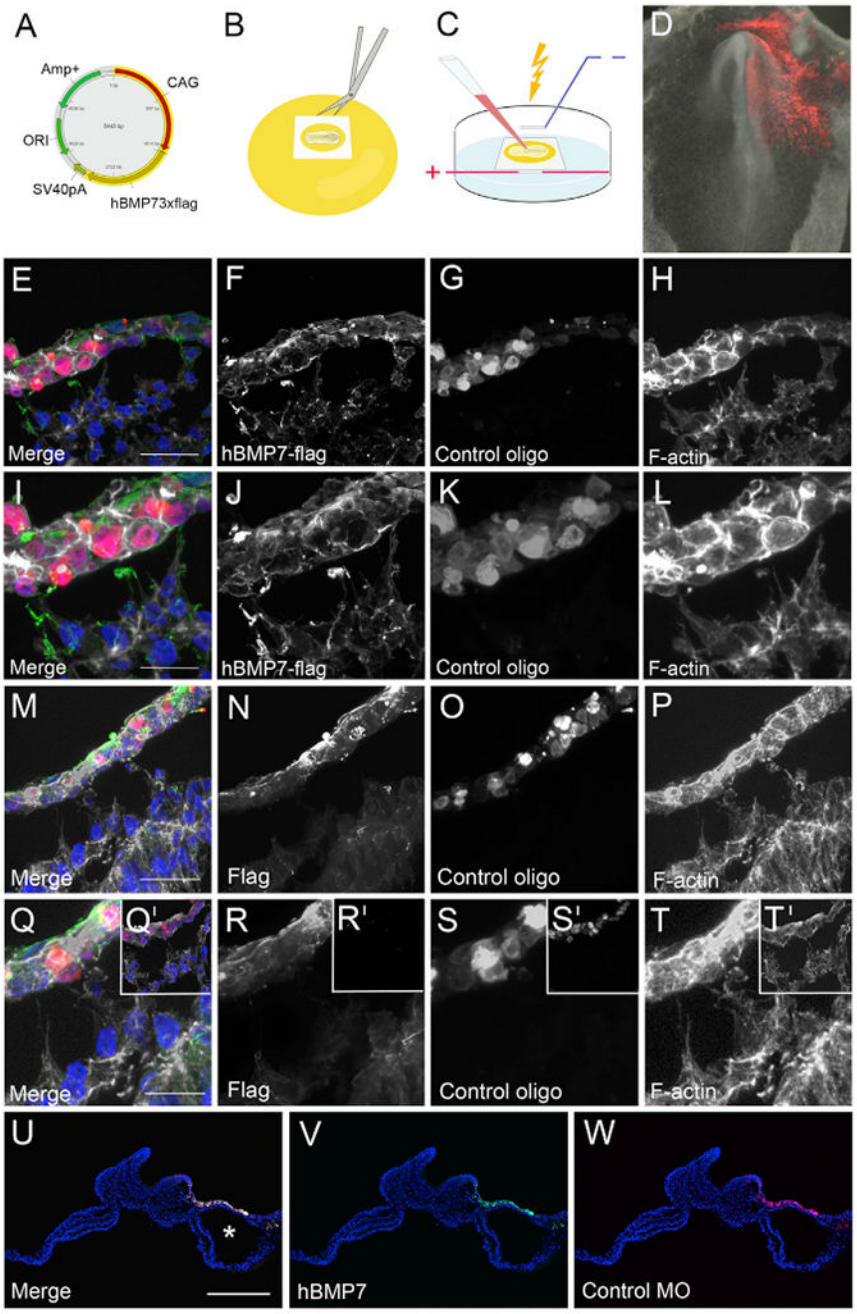

Figure 3. Mesodermal Cell Projections Receive BMP7 from the Ectoderm

(A) Construct expressing human BMP7 that carries a triple FLAG tag was used.

(B) Chick embryos were cultivated on a filter paper.

(C) hBMP7 construct was electroporated into the ectoderm *ex ovo*.

(D) Fluorescently labeled control oligo shows the area of transfection (n = 10).

(E) Red label of the control oligo is in the ectoderm, and green label of the FLAG tag is in the ectoderm and mesoderm. White staining represents F-actin deposition, and nuclei are in blue. Scale bar: 20 μm.

(F) Single channel for FLAG tag shows distribution in ectoderm and mesoderm.
(G) Single channel for transfection control oligo, which is only present in the ectoderm.
(H) Single channel for F-actin.
(I) Higher magnification reveals that actin-containing mesodermal cell projections carry the FLAG-tagged hBMP7 protein. Scale bar: 10 μm.
(J–L) Single channels for FLAG tag, transfection control morpholino, and F-actin, respectively, as indicated.
(M) Overexpression of control vector expressing a triple FLAG tag (green) in the ectoderm (n = 9). Exclusive ectodermal transfection is demonstrated by control oligo co-transfection in red. Mesodermal cell projections extend toward ectoderm but do not take up the FLAG tag. Scale bar: 20 μm.
(N–P) Single channels, as in (J)–(L).
(Q–T) Higher magnification reveals cell projections that have not received the FLAG tag expressed in the ectoderm. Scale bar: 10 μm. Fluorescent signals are as indicated. (Q′–T′) Negative control of anti-FLAG staining on tissue section treated with control morpholino without anti-FLAG primary antibody.
(U–W) Overexpression of hBMP7 in the overlying ectoderm leads to enhanced body cavity formation (asterisk) (n = 6). Fluorescent signals are as indicated. Scale bar: 200 μm.
See also Figures S1 and S2.

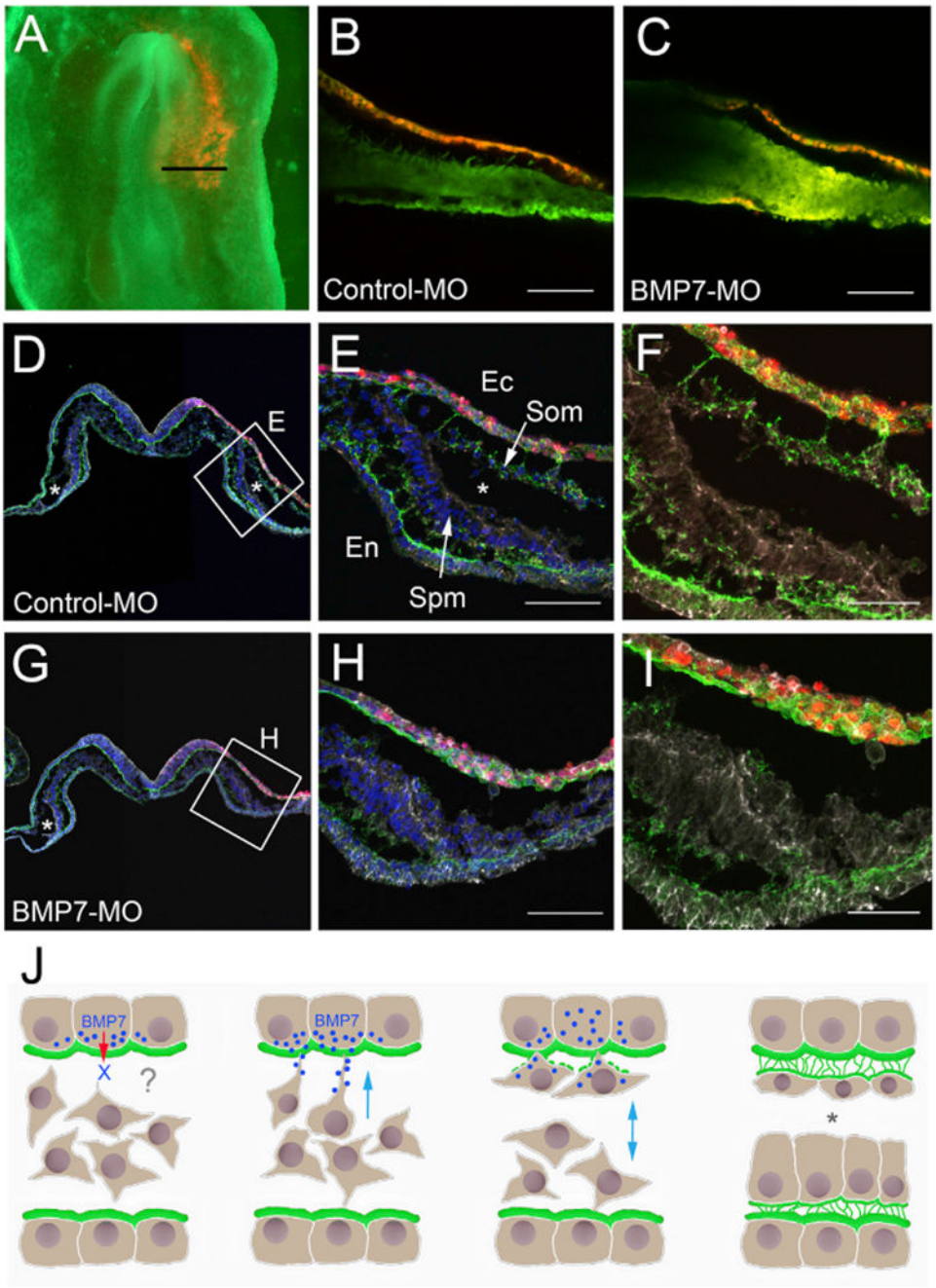

Figure 4. Suppression of BMP7 in the Ectoderm Diminishes Body Cavity Development

(A) The ectoderm of a GFP-expressing embryo transfected with a red labelled morpholino.

(B) Single image of live imaging analysis of GFP-expressing embryo with a red control morpholino (Scale bar in B,C: 50μm).

(C) Ectoderm transfection with a red labelled morpholino against BMP7 leads to a reduction of mesodermal cell projections towards the ectoderm.

(D) Montage of left and right side of an embryo section transfected with a red control morpholino in the ectoderm and stained for Laminin1 in green and F-actin in white. The body cavity has been formed (asterisk) (n= 24), Scale bar: 150μm.
(E) Subarea of D in which body cavity formation has occurred (asterisk) and two separate epithelial mesodermal layers have been established. Somatic mesodermal cells display interactions with the ectodermal basal lamina by forming long cell projections which are intertwined with Laminin1 (Scale bar: 80μm).
(F) Higher magnification without DAPI to enhance visualization of the fine filamentous cell interaction and the network of Laminin1 (Scale bar: 40μm).
(G) Transfection with a morpholino directed against BMP7 (n=18). Body cavity formation is not discernable (Scale bar: 150μm) (montage of left and right side).
(H) Subarea magnification reveals the lack of Laminin1 deposition in the dorsal mesoderm and the lack of cell projections towards the ectoderm. The mesoderm did not form two separate epithelialized layers (unpaired t-test control vs morpholino, p-value < 0,001), scale bar: 80μm.
(I) Lack of mesodermal cell projections, lack of Laminin1 deposition and absence of tissue interaction between ectoderm and mesoderm (scale bar: 40μm).
(J) Model for body cavity formation. 1 - BMP7 is expressed in the ectoderm overlying the native lateral plate mesoderm. 2 - Mesodermal cells are attracted to the ectoderm and form cell projections by which they interact with ectodermal cells and directly take up ectodermal BMP7. It is currently unknown if BMP is acting directly or indirectly in attracting mesodermal cells. 3 - The native mesoderm population is separated into dorsal and ventral subpopulations. 4 - Polarization and epithelialization to form the body cavity (asterisk).
Ec: ectoderm, En: endoderm, Som: somatic mesoderm, Spm: splanchnic mesoderm. See also Figures S3 and S4 and Videos S3 and S4.